

Unusual electronic structure of Dirac material $BaMnSb_2$ revealed by angle-resolved photoemission spectroscopy

Hongtao Rong(戎洪涛), Liqin Zhou(周丽琴), Junbao He(何俊宝), Chunyao Song(宋春尧), Yu Xu(徐煜), Yongqing Cai(蔡永青), Cong Li(李聪), Qingyan Wang(王庆艳), Lin Zhao(赵林), Guodong Liu(刘国东), Zuyan Xu(许祖彦), Genfu Chen(陈根富), Hongming Weng(翁红明), and Xingjiang Zhou(周兴江)

Citation: Chin. Phys. B, 2021, 30 (**6**): 067403. DOI: 10.1088/1674-1056/ac0036
Journal homepage: http://cpb.iphy.ac.cn; http://iopscience.iop.org/cpb

What follows is a list of articles you may be interested in

Evidence for bosonic mode coupling in electron dynamics of LiFeAs superconductor

Cong Li(李聪), Guangyang Dai(代光阳), Yongqing Cai(蔡永青), Yang Wang(王阳), Xiancheng Wang(望贤成), Qiang Gao(高强), Guodong Liu(刘国东), Yuan Huang(黄元), Qingyan Wang(王庆艳), Fengfeng Zhang(张丰丰), Shenjin Zhang(张申金), Feng Yang(杨峰), Zhimin Wang(王志敏), Qinjun Peng(彭钦军), Zuyan Xu(许祖彦), Changqing Jin(靳常青), Lin Zhao(赵林)†, and X J Zhou(周兴江)‡

Chin. Phys. B, 2020, 29 (**10**): 107402. DOI: 10.1088/1674-1056/abb21f

Electronic structure and spatial inhomogeneity of iron-based superconductor FeS

Chengwei Wang(王成玮), Meixiao Wang(王美晓), Juan Jiang(姜娟), Haifeng Yang(杨海峰), Lexian Yang(杨乐仙), Wujun Shi(史武军), Xiaofang Lai(赖晓芳), Sung-Kwan Mo, Alexei Barinov, Binghai Yan(颜丙海), Zhi Liu(刘志), Fuqiang Huang(黄富强), Jinfeng Jia(贾金峰), Zhongkai Liu(柳仲楷), Yulin Chen(陈宇林)

Chin. Phys. B, 2020, 29 (**4**): 047401. DOI: 10.1088/1674-1056/ab75d4

Electronic structure and nematic phase transition in superconducting multiple-layer FeSe films grown by pulsed laser deposition method

Bing Shen(沈兵), Zhong-Pei Feng(冯中沛), Jian-Wei Huang(黄建伟), Yong Hu(胡勇), Qiang Gao(高强), Cong Li(李聪), Yu Xu(徐煜), Guo-Dong Liu(刘国东), Li Yu(俞理), Lin Zhao(赵林), Kui Jin(金魁), X J Zhou(周兴江)

Chin. Phys. B, 2017, 26 (**7**): 077402. DOI: 10.1088/1674-1056/26/7/077402

Electronic structure of heavy fermion system $CePt_2In_7$ from angle-resolved photoemission spectroscopy

Bing Shen(沈兵), Li Yu(俞理), Kai Liu(刘凯), Shou-Peng Lyu(吕守鹏), Xiao-Wen Jia(贾小文), E D Bauer, J D Thompson, Yan Zhang(张艳), Chen-Lu Wang(王晨露), Cheng Hu(胡成), Ying Ding(丁颖), Xuan Sun(孙璇), Yong Hu(胡勇), Jing Liu(刘静), Qiang Gao(高强), Lin Zhao(赵林), Guo-Dong Liu(刘国东), Zu-Yan Xu(许祖彦), Chuang-Tian Chen(陈创天), Zhong-Yi Lu(卢仲毅), X J Zhou(周兴江)

Chin. Phys. B, 2017, 26 (**7**): 077401. DOI: 10.1088/1674-1056/26/7/077401

Angle-resolved photoemission spectroscopy study on iron-based superconductors

Ye Zi-Rong, Zhang Yan, Xie Bin-Ping, Feng Dong-Lai

Chin. Phys. B, 2013, 22 (**8**): 087407. DOI: 10.1088/1674-1056/22/8/087407

RAPID COMMUNICATION

Unusual electronic structure of Dirac material $BaMnSb_2$ revealed by angle-resolved photoemission spectroscopy*

Hongtao Rong(戎洪涛)[1,2,†], Liqin Zhou(周丽琴)[1,2,†], Junbao He(何俊宝)[1,2,3,†], Chunyao Song(宋春尧)[1,2,†], Yu Xu(徐煜)[1,2], Yongqing Cai(蔡永青)[1,2], Cong Li(李聪)[1,2], Qingyan Wang(王庆艳)[1,2], Lin Zhao(赵林)[1,2,4], Guodong Liu(刘国东)[1,2,4], Zuyan Xu(许祖彦)[5], Genfu Chen(陈根富)[1,2], Hongming Weng(翁红明)[1,2], and Xingjiang Zhou(周兴江)[1,2,4,6,‡]

[1] *National Laboratory for Superconductivity, Beijing National Laboratory for Condensed Matter Physics, Institute of Physics, Chinese Academy of Sciences, Beijing* 100190, *China*

[2] *University of Chinese Academy of Sciences, Beijing* 100049, *China*

[3] *Henan International Joint Laboratory of MXene Materials Microstructure, College of Physics and Electronic Engineering, Nanyang Normal University, Nanyang* 473061, *China*

[4] *Songshan Lake Materials Laboratory, Dongguan* 523808, *China*

[5] *Technical Institute of Physics and Chemistry, Chinese Academy of Sciences, Beijing* 100190, *China*

[6] *Beijing Academy of Quantum Information Sciences, Beijing* 100193, *China*

(Received 7 May 2021; revised manuscript received 7 May 2021; accepted manuscript online 12 May 2021)

High resolution angle resolved photoemission measurements and band structure calculations are carried out to study the electronic structure of $BaMnSb_2$. All the observed bands are nearly linear that extend to a wide energy range. The measured Fermi surface mainly consists of one hole pocket around Γ and a strong spot at Y which are formed from the crossing points of the linear bands. The measured electronic structure of $BaMnSb_2$ is unusual and deviates strongly from the band structure calculations. These results will stimulate further efforts to theoretically understand the electronic structure of $BaMnSb_2$ and search for novel properties in this Dirac material.

Keywords: ARPES, $BaMnSb_2$, Dirac material, magnetic topological material

PACS: 74.25.Jb **DOI:** 10.1088/1674-1056/ac0036

Topological materials, including topological insulators, topological semimetals, and topological superconductors, have attracted much attention due to their unique electronic structure, exotic physical properties, and potential applications.[1–7] Magnetic topological materials, with the introduction of magnetism to break the time-reversal symmetry, can generate novel topological phases such as the quantum anomalous Hall state.[8–15] The $AMnPn_2$ (A = Ca, Sr, Ba, Eu or Yb; Pn = Bi or Sb) family has provided a desirable platform to search for intrinsic magnetic topological materials.[16–26] In these materials, the Bi or Sb layer can host Dirac dispersion and the Mn sublattice can provide magnetic environment. The introduction of Eu or Yb on the A site can further manipulate the magnetic structure in the system. In addition to the magnetic structure, it has been found that the electronic structure and topological properties also depend sensitively on the crystal structure.[27] Among all the compounds in the $AMnPn_2$ family, $BaMnSb_2$ is unique because it has a crystal structure that is distinct from other members in the family. While there have been some investigations on $BaMnSb_2$,[21,24,28–30] the detailed study of its electronic structure is still limited.[21,24]

In this paper, we have carried out detailed high resolution angle resolved photoemission spectroscopy (ARPES) measurements and band structure calculations to study the electronic structure of $BaMnSb_2$. The observed Fermi surface mainly consists of one hole pocket around Γ and a strong spot at Y. The measured band structures are dominated by nearly linear bands that extend to a wide energy range. The measured electronic structures are unusual which deviate obviously from the band structure calculations.

High-quality single crystals of $BaMnSb_2$ were grown by flux method.[31] The elements Ba, Mn, and Sb were mixed in

*Project supported by the National Key Research and Development Program of China (Grant Nos. 2016YFA0300600, 2018YFA0305602, 2016YFA0300300, and 2017YFA0302900), the National Natural Science Foundation of China (Grant Nos. 11974404, 11888101, 11922414, and 11404175), the Strategic Priority Research Program (B) of the Chinese Academy of Sciences (Grant Nos. XDB33000000 and XDB25000000), the Youth Innovation Promotion Association of CAS (Grant No. 2017013), and the Natural Science Foundation of Henan Province, China (Grant Nos. 182300410274 and 202300410296). The theoretical calculations are supported by the National Natural Science Foundation of China (Grant Nos. 11674369, 11865019, and 11925408), the Beijing Natural Science Foundation, China (Grant No. Z180008), Beijing Municipal Science and Technology Commission, China (Grant No. Z191100007219013), the National Key Research and Development Program of China (Grant Nos. 2016YFA0300600 and 2018YFA0305700), the K. C. Wong Education Foundation (Grant No. GJTD-2018-01), and the Strategic Priority Research Program of Chinese Academy of Sciences (Grant No. XDB33000000).

†These authors contributed equally.

‡Corresponding author. E-mail: xjzhou@iphy.ac.cn

© 2021 Chinese Physical Society and IOP Publishing Ltd

the ratio of Ba : Mn : Sb = 1 : 1 : 4, put into an alumina crucible, and sealed in a quartz tube. The quartz tube was heated slowly to 900 °C, held for 20 hours, and then cooled to 700 °C at a rate of 1 °C/hour, where the excess flux was removed using a centrifuge. Shiny platelike single crystals with a typical dimension of $5 \times 5 \times 1$ mm^3 were obtained. We carried out single crystal x-ray diffraction to analyze the crystal structure of the samples at 273 K. It crystalizes in an orthorhombic structure (space group: *Imm*2) with lattice constants $a =$ 24.258 Å, $b = 4.4827$ Å, and $c = 4.506$ Å, consistent with the previous reports.[21,24] ARPES measurements were performed at our lab-ARPES system equipped with 21.218 eV Helium discharge lamp and Scienta DA30L electron energy analyzer.[32,33] The energy resolution was set at ~ 20 meV. The angular resolution was $\sim 0.3°$. The Fermi level is referenced by measuring on the Fermi edge of a clean polycrystalline gold that is electrically connected to the sample. All the samples were cleaved *in situ* and measured in ultrahigh vacuum with a base pressure better than 5×10^{-11} mbar.

The first-principle calculations to simulate the electronic structures of $BaMnSb_2$ were implemented by using the Vienna *ab initio* simulation package (VASP).[34] The generalized gradient approximation (GGA) of the Perdew–Burke–Ernzerhof (PBE) type was selected to describe the exchange–correlation function.[35] The Brillouin zone (BZ) integration was sampled by $3 \times 11 \times 11$ k mesh and the cut-off energy was set to 500 eV. Spin–orbital coupling (SOC) was taken into account. The tight-binding model of $BaMnSb_2$ was constructed by using the Wannier90 with Ba 5d orbitals, Sb 5p orbitals, and Mn 3d orbitals, which is based on the maximally-localized Wannier functions (MLWF).[36] The bulk Fermi surfaces of $BaMnSb_2$ were calculated by the WannierTools package.[37]

The crystal structure of $BaMnSb_2$ is shown in Fig. 1(a). It consists of an alternate stacking of $MnSb_4$ layer and Ba–Sb–Ba layer along the a axis. In the central Ba–Sb–Ba layer, the Sb atoms in the Sb sheet form zig-zag chains with the chain direction along the b axis (Fig. 1(b)). The Ba atoms above and below the Sb sheet are coincident. Figure 1(c) shows the measured Fermi surface mapping of $BaMnSb_2$ at 30 K. The main features observed consist of a circular Fermi surface sheet around Γ and a strong spot at Y. No features are observed at X. Figure 1(d) shows the constant energy contours at different binding energies. At low binding energies below ~ 100 meV, one circle can be observed around Γ. When the binding energy is higher than ~ 200 meV, combined with the detailed band structure analysis near Γ (Fig. 2) and near Y (Fig. 3), three main features appear around Γ: an outer sheet α, an inner vertical ellipse β, and another inner horizontal ellipse γ. With increasing binding energy, the outer α sheet increases in its area significantly while the two inner ellipses β and γ get elongated along their long axis. In the mean time, as seen in Fig. 1(d), the feature at Y stays as a strong spot up to the binding energy of ~ 200 meV and it disintegrates at higher binding energies.

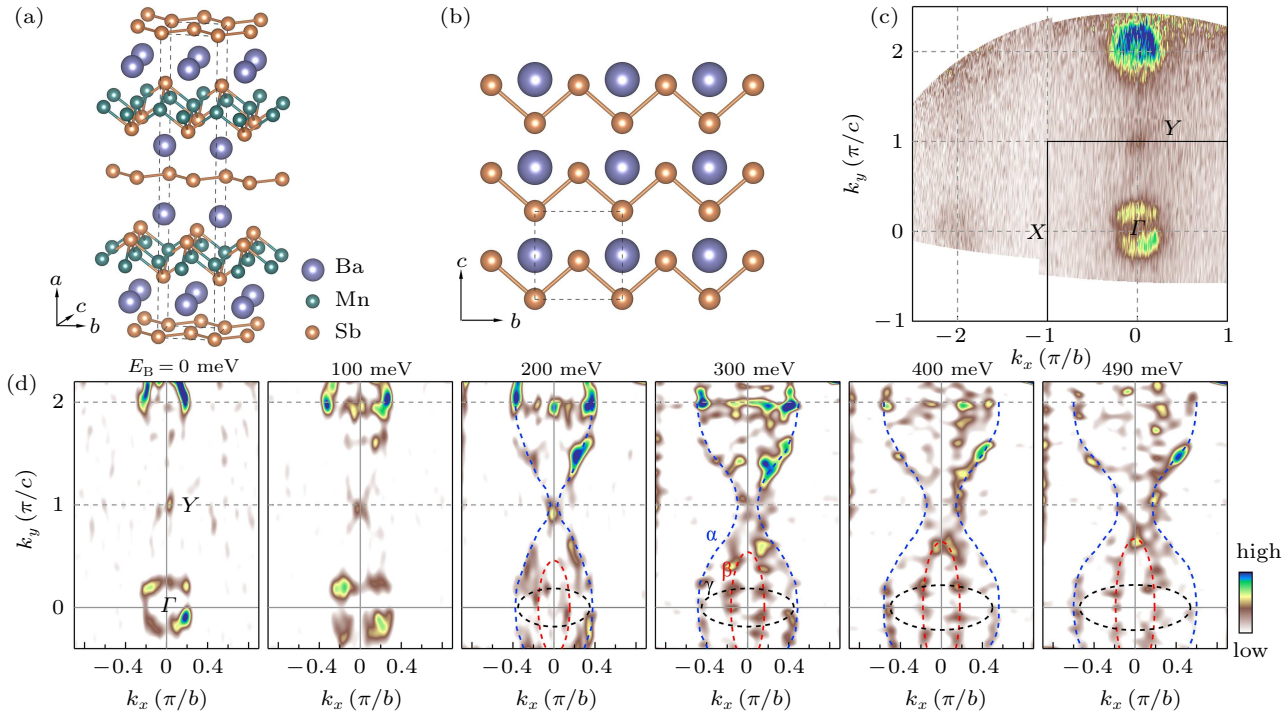


Fig. 1. Fermi surface mapping and constant energy contours of $BaMnSb_2$. (a) Crystal structure of $BaMnSb_2$. The unit cell is indicated by the black dashed lines. (b) Top view of the central Ba–Sb–Ba layer which consists of the zig-zag chainlike structure along the b axis in the Sb layer. (c) Fermi surface mapping obtained by integrating the photoemission spectral weight over a $[-20, 20]$ meV energy window with respect to the Fermi level. (d) Constant energy contours at different binding energies of 0 meV, 100 meV, 200 meV, 300 meV, 400 meV, and 490 meV. These are second derivative images obtained by integrating the spectral weight over a $[-20, 20]$ meV energy window with respect to each binding energy.

In Fig. 2, we zoom in onto the detailed electronic structure around Γ point in $BaMnSb_2$. Figures 2(a)–2(d) show the band structures measured along different momentum cuts around Γ. In all these measurements, mainly two sets of bands are observed, labeled as α and β bands in Fig. 2(b) for the cut 6 along the Γ–X direction and labeled as β and γ bands in Fig. 2(d) for the cut 12 along the Γ–Y direction. These α, β, and γ bands are nearly linear in dispersion that extend to a wide energy range up to 0.9 eV (Fig. 2(b)). As seen in Figs. 2(a) and 2(b) for the momentum cuts parallel to Γ–X, the β band is very steep; the corresponding Fermi velocity is $\sim$ 13 eV·Å for the β band in Fig. 2(b). The two linear bands α and β intersect, as shown in Figs. 2(a) and 2(b), and the energy position of the crossing point varies for different momentum cuts. For the momentum cuts 4 to 8, we find that the crossing point is closed the Fermi level. These Dirac cone-like bands give rise to the formation of the hole-like Fermi surface around Γ as shown in Fig. 2(e). When the momentum cuts move away further from Γ (cuts 1–3 and cuts 9–11), the crossing point of the α and β bands shifts down from the Fermi level and the spectral weight at the Fermi level gets depleted. The α and β bands observed in Fig. 2 contribute to the formation of the α and β sheets in the constant energy contours at high binding energies above 200 meV in Fig. 1(d). The band structure for the cut 12 along the Γ–Y direction, shown in Fig. 2(d), also consists of two main bands around Γ. In this case, combined with the constant energy contours in Fig. 1(d), the outer band can be assigned to β that forms the β sheet in Fig. 1(d) while the inner γ band contributes to the formation of the γ sheet in Fig. 1(d). In addition to the main linear bands α and β, there is another band observed in the measured band structure for the momentum cut 6 along the Γ–X direction (Fig. 2(c)). This band is flat; it does not show up in the MDC second derivative image in Fig. 2(b) but becomes clear in the EDC second derivative image in Fig. 2(c). The band lies about 130 meV below the Fermi level. The combined MDC and EDC second derivative analyses provide a complete picture of the band structure around Γ (Figs. 2(a)–2(c)).

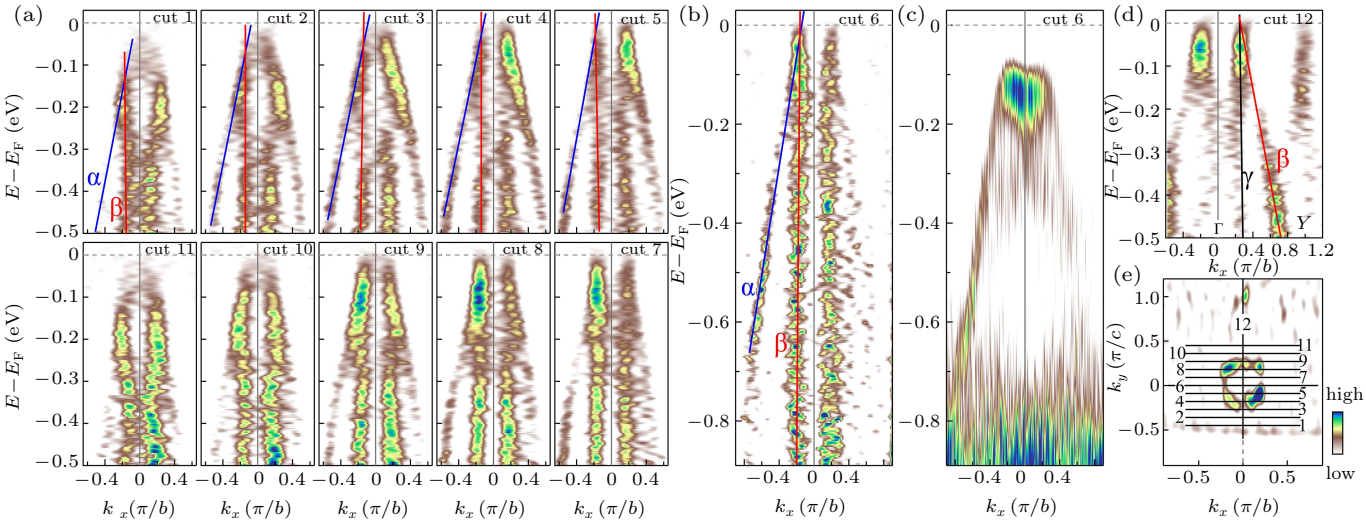


Fig. 2. Hole-like Fermi surface and detailed band structures of $BaMnSb_2$ around Γ measured at 30 K. (a)–(b) Band structure measured along the Γ–X direction for various momentum cuts at different k_ys. These are the second derivative images with respect to momentum. The location of the momentum cuts, cut 1 to cut 11, is marked by black lines in (e). (c) Band structure for momentum cut 6. It is the second derivative image with respect to energy. (d) Band structure for momentum cut 12; its location is marked by black line in (e). It is the second derivative image with respect to momentum. (e) Fermi surface mapping around Γ. It is the second derivative image obtained by integrating the spectral weight over a [−20, 20] meV energy window with respect to the Fermi level.

Figure 3 shows the zoomed-in constant energy contours and the detailed electronic structures of $BaMnSb_2$ around the Y point. In all the bands measured along different momentum cuts around Y in Figs. 3(d) and 3(e), we observe mainly one set of bands, named as δ in Fig. 3(e). These δ bands are nearly linear over a large energy range ($\sim$ 0.9 eV in Fig. 3(e)). For the momentum cut 6 along the Y–M direction, the two linear bands have a Fermi velocity of $\sim$ 2.9 eV·Å and cross each other near the Fermi level (Fig. 3(e)). When the momentum cuts move away from cut 6 (cut 1 to cut 5 and cut 7 to cut 11 in Fig. 3(d)), the spectral weight gets suppressed more and more below the Fermi level. Such a momentum-dependent band evolution produces a strong spot at Y in the measured Fermi surface (Fig. 3(a)) and the evolution of the constant energy contours around Y as shown in Figs. 1(d), 3(b), and 3(c). In addition to the main linear bands, there is another band observed in the measured band structure for the momentum cut 6 along the Y–M direction (Fig. 3(f)). This band is hole-like with its top at $\sim$ 300 meV. It does not show up in the MDC second derivative image in Fig. 3(e) but becomes visible in the EDC second derivative image in Fig. 3(f).

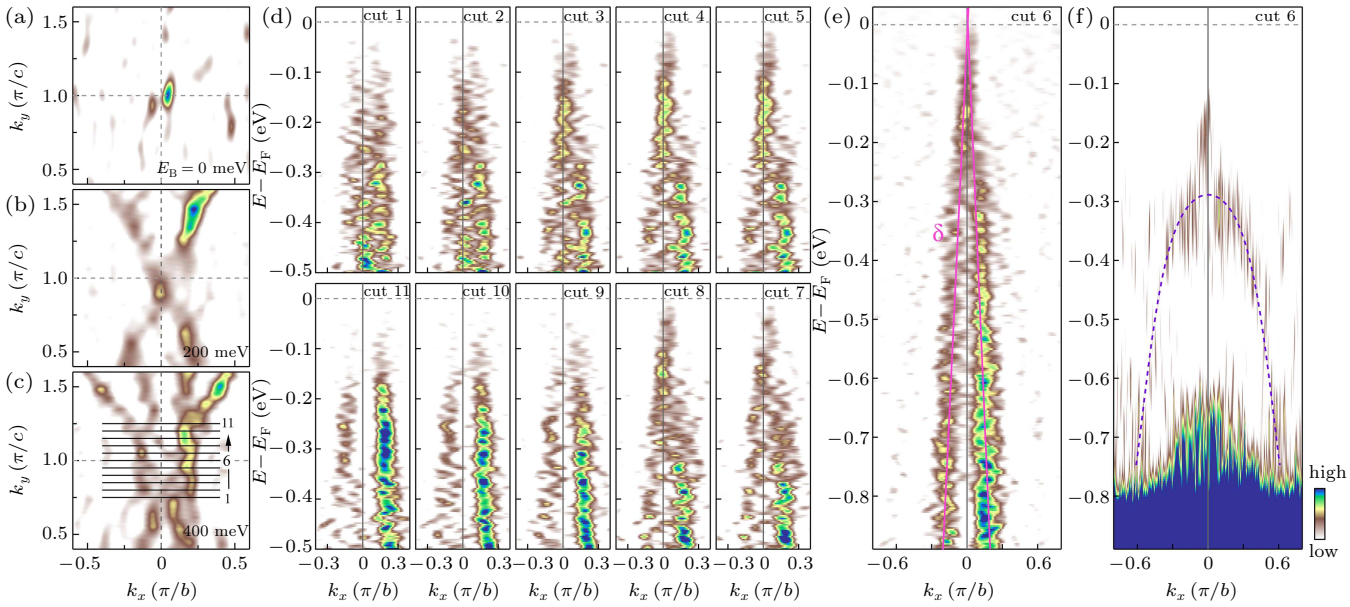


Fig. 3. Fermi surface mapping and detailed band structures of $BaMnSb_2$ around Y measured at 30 K. (a)–(c) Constant energy contours at binding energies of 0 meV (a), 200 meV (b), and 400 meV (c). These are second derivative images obtained by integrating the spectral weight over a [−20, 20] meV energy window at binding energies of 0 meV, 200 meV, and 400 meV. (d)–(e) Band structure measured along the Γ–X direction for various momentum cuts at different k_ys. These are the second derivative images with respect to momentum. The location of the momentum cuts, cut 1 to cut 11, is marked by black lines in (a). (f) Band structure for momentum cut 6. It is the second derivative image with respect to energy.

In order to understand our measured results, we carried out detailed band structure calculations of $BaMnSb_2$ as shown in Fig. 4. In the calculations, we took a G-type magnetic structure in $BaMnSb_2$ (Fig. 4(a)) where both the interlayer and intralayer couplings between two nearest moments in the $MnSb_4$ layer are antiferromagnetic.[28] Figure 4(c) shows the overall calculated band structure of $BaMnSb_2$ without considering the spin–orbital coupling (SOC). The low energy band structure near the Γ point mainly consists of two M-shaped bands. The band structure near the Y point is dominated by a cusp structure below the Fermi level and a dip structure above the Fermi level. The position of the cusp and dip structures deviates from the Y point along the Y–M direction. Even without considering SOC, there is a prominent gap between the dip and the cusp which is about 380 meV. When SOC is taken into account in the band structure calculations, overall it causes the lifting of the band degeneracy and band splitting as seen in Figs. 4(d) and 4(e). The effect of SOC on the low energy band structure near the Γ point is small but dramatic changes of the band structure occur near the Y point (Figs. 4(d) and 4(e)). The initial one band of the cusp and dip structures in Fig. 4(c) splits into multiple bands. In the meantime, both structures move towards the Fermi level and develop into a Dirac cone-like band with a much reduced gap of $\sim$ 130 meV. The low energy electronic structure of $BaMnSb_2$ is rather two-dimensional. When k_z moves from 0 (Fig. 4(d)) to π/a (Fig. 4(e)), the bands near the Y point are barely changed, although there is a slight change in the bands near the Γ point.

Now we compare the calculated and measured electronic structures of $BaMnSb_2$. Figures 5(a) and 5(b) compare the calculated (Fig. 5(a)) and measured (Fig. 5(b)) band structures along several high symmetry directions. Figures 5(c)–5(f) compare the calculated (Figs. 5(c) and 5(d)) and measured (Figs. 5(e) and 5(f)) Fermi surface and constant energy contour. Considering the observation of the feature at Y, an experimental Fermi level $E_{F(exp)}$ is taken which is 0.16 eV below the Fermi level in the calculation as show in Fig. 5(a). The measured electronic structure of $BaMnSb_2$ shows some consistence with the calculations on a few main aspects. The first is the hole like bands around Γ and Dirac-like band around Y (Figs. 5(a) and 5(b)). Second, the Fermi surface consists of the hole like sheet around Γ and some peculiar features around Y (Figs. 5(c) and 5(e)). Third, the observed features in the measured constant energy contour (Fig. 5(f))) show some resemblance to those in the calculated constant energy contour (Fig. 5(d)). However, the overall calculated electronic structure shows some strong deviations from the measured results. First, the number of the observed bands is much less than that of the calculated bands both around the Γ and Y points. Second, the observed bands are nearly linear that extend to a large energy range of $\sim$ 0.9 eV (Fig. 5(b)). It is hard to find the corresponding bands in the calculations (Fig. 5(a)). Third, although there are some similarities in the calculated and measured Fermi surface and constant energy contours, there remain significant differences on the size of the Fermi surface and the features in the constant energy contour. In some other compounds like $SrMnBi_2$, $CaMnBi_2$, and $CaMnSb_2$, the measured electronic structure is found to be in excellent agreement with the band structure calculations.[17,27] The measured electronic structure of $BaMnSb_2$ is unusual that it can not be described properly by the band structure calculations.

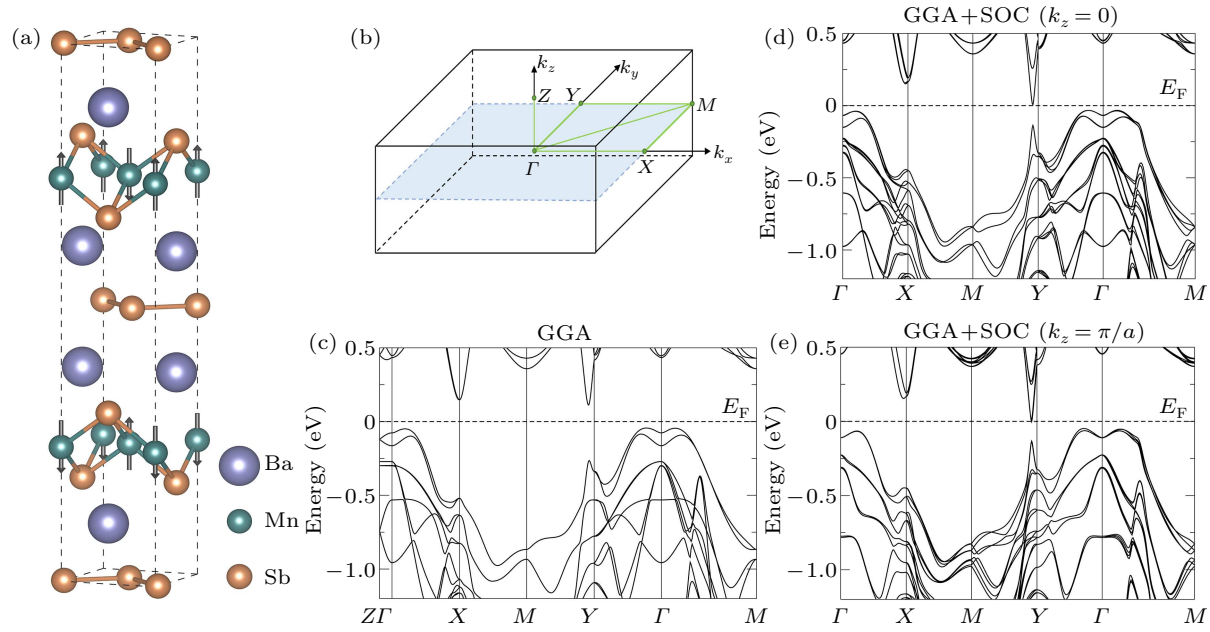


Fig. 4. Calculated band structures of $BaMnSb_2$. (a) Magnetic structure of $BaMnSb_2$. (b) Three-dimensional Brillouin zone of $BaMnSb_2$. Green lines indicate high symmetry directions. (c)–(d) Calculated band structure of $BaMnSb_2$ without (c) and with (d) spin–orbit coupling at $k_z = 0$. (e) Calculated band structure with spin–orbit coupling at $k_z = \pi/a$.

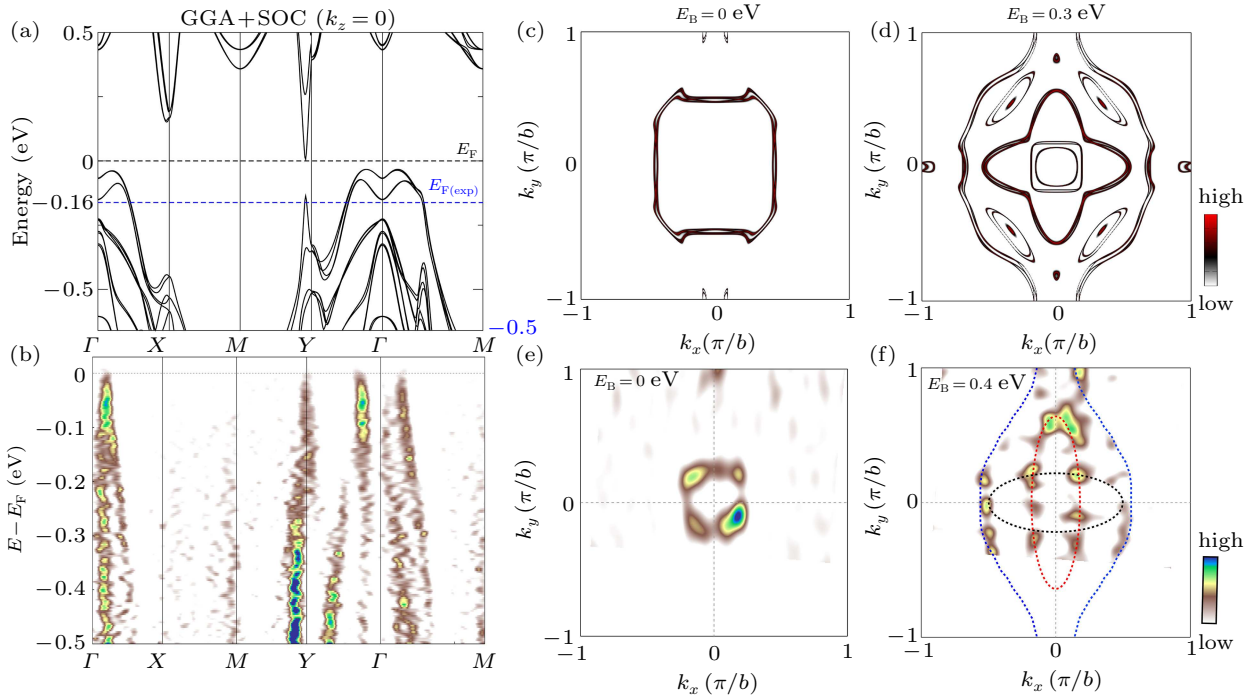


Fig. 5. Comparison between the calculated and measured electronic structures of $BaMnSb_2$. (a) Calculated band structure of $BaMnSb_2$ with spin–orbit coupling at $k_z = 0$. (b) Measured band structure of $BaMnSb_2$. This is the second derivative image with respect to the momentum. (c)–(d) Calculated Fermi surface (c) and constant energy contour at a binding energy of 0.3 eV (d). (e)–(f) Measured Fermi surface (e) and constant energy contour at a binding energy of 0.4 eV (f). These are second derivative images obtained by integrating the spectral weight over a [−20, 20] meV energy window with respect to each binding energy.

In summary, we have carried out detailed high resolution ARPES measurements and band structure calculations to study the electronic structure of $BaMnSb_2$. The measured electronic structure of $BaMnSb_2$ is unusual in three aspects. First, all the measured bands are nearly linear that extend to a wide energy range. Second, the observed Fermi surface mainly consists of one hole pocket around Γ and a strong spot at Y. The Fermi surface is formed from the crossing points of the linear bands. Third, the measured electronic structure deviates strongly from the band structure calculations. These results will stimulate further efforts to theoretically understand the electronic structure of $BaMnSb_2$ and search for novel properties in this Dirac material.

References

[1] Hasan M Z and Kane C L 2010 *Rev. Mod. Phys.* **82** 3045
[2] Qi X L and Zhang S C 2011 *Rev. Mod. Phys.* **83** 1057
[3] Bansil A, Lin H and Das T 2016 *Rev. Mod. Phys.* **88** 021004
[4] Fang C, Weng H M, Dai X and Fang Z 2016 *Chin. Phys. B* **25** 117106
[5] Yan B H and Felser C 2017 *Annu. Rev. Condens. Matter. Phys.* **8** 337
[6] Armitage N P, Mele E J and Vishwanath A 2018 *Rev. Mod. Phys.* **90** 015001
[7] Tokura Y, Yasuda K and Tsukazaki A 2019 *Nat. Rev. Phys.* **1** 126
[8] Qi X L, Hughes T L and Zhang S C 2008 *Phys. Rev. B* **78** 195424
[9] Wan X G, Turner A M, Vishwanath A and Savrasov S Y 2011 *Phys. Rev. B* **83** 205101
[10] Yu R, Zhang W, Zhang H J, Zhang S C, Dai X and Fang Z 2010 *Science* **329** 61
[11] Chang C Z, Zhang J S, Feng X, *et al.* 2013 *Science* **340** 167
[12] Otrokov M M, Klimovskikh I I, Bentmann H, *et al.* 2019 *Nature* **576** 416
[13] Gong Y, Guo J W, Li J H, *et al.* 2019 *Chin. Phys. Lett.* **36** 076801
[14] Zhang D Q, Shi M J, Zhu T S, *et al.* 2019 *Phys. Rev. Lett.* **122** 206401
[15] Xu Y F, Elcoro L, Song Z D, *et al.* 2020 *Nature* **586** 702
[16] Park J, Lee G, Wolff-Fabris F, *et al.* 2011 *Phys. Rev. Lett.* **107** 126402
[17] Feng Y, Wang Z J, Chen C Y, *et al.* 2014 *Sci. Rep.* **4** 5385
[18] Kealhofer R, Jang S, Griffin S M, *et al.* 2018 *Phys. Rev. B* **97** 045109
[19] Ramankutty S V, Henke J, Schiphorst A, *et al.* 2018 *SciPost Phys.* **4** 010
[20] Ryu H, Park S Y, Li L J, *et al.* 2018 *Sci. Rep.* **8** 15322
[21] Sakai H, Fujimura H, Sakuragi S, *et al.* 2020 *Phys. Rev. B* **101** 081104(R)
[22] Borisenko S, Evtushinsky D, Gibson Q, *et al.* 2019 *Nat. Commun.* **10** 3424
[23] Soh J R, Manuel P, Schröter N M B, *et al.* 2019 *Phys. Rev. B* **100** 174406
[24] Liu J Y, Yu J, Ning J L, *et al.* 2019 arXiv: 1907.06318
[25] Liu J Y, Hu J, Zhang Q, *et al.* 2017 *Nat. Mat.* **16** 905
[26] Masuda H, Sakai H, Tokunaga M, *et al.* 2016 *Sci. Adv.* **2** e1501117
[27] Rong H T, Zhou L Q, He J B, *et al.* 2021 arXiv: 2105.00444
[28] Liu J Y, Hu J, Cao H B, *et al.* 2016 *Sci. Rep.* **6** 30525
[29] Huang S L, Kim J, Shelton W A, *et al.* 2017 *Proc. Natl. Acad. Sci.* **114** 6256
[30] Yu J B and Liu C X 2020 *Nat. Commun.* **11** 2290
[31] He J B, Fu Y, Zhao L X, *et al.* 2017 *Phys. Rev. B* **95** 045128
[32] Liu G D, Wang G L, Zhu Y, *et al.* 2008 *Rev. Sci. Instrum.* **79** 023105
[33] Zhou X J, He S L, Liu G D, *et al.* 2018 *Rep. Prog. Phys.* **81** 062101
[34] Kresse G and Furthmüller J 1996 *Phys. Rev. B* **54** 11169
[35] Perdew J P, Burke K and Ernzerhof M 1996 *Phys. Rev. Lett.* **77** 3865
[36] Mostofi A A, Yates J R, Pizzi G, *et al.* 2014 *Comput. Phys. Commun.* **185** 2309
[37] Wu Q S, Zhang S N, Song H F, *et al.* 2018 *Comput. Phys. Commun.* **224** 405